RAPID COMMUNICATIONS

PHYSICAL REVIEW B VOLUME 33, NUMBER 8 15 APRIL 1986

Folded acoustic phonons in Si-Si_xGe_{1-x} superlattices

H. Brugger and G. Abstreiter
Physik-Department E 16, Technische Universität München, D-8046 Garching, Federal Republic of Germany

H. Jorke, H. J. Herzog, and E. Kasper
Forschungsinstitut, Allgemeine Elektrizitäts-Gesellschaft Telefunken, D-7900 Ulm, Federal Republic of Germany

(Received 6 December 1985)

Raman scattering from folded longitudinal acoustic phonons in Si-Si_xGe_{1-x} superlattices is observed. The measured phonon energies are explained by use of the elastic continuum theory for the acoustic modes. This leads to an accurate determination of the superlattice period.

Recently, Si-Si_xGe_{1-x} strained-layer superlattices have received considerable attention. This is mainly caused by the achievement of high-quality pseudomorphic growth of multilayer structures by silicon molecular-beam epitaxy.[1-3] Enhanced mobilities of two-dimensional electron and hole gases have been reported in selectively doped samples.[4,5] These successful experiments have stimulated discussions on novel electronic and optoelectronic devices based on Si-Si_xGe_{1-x} multiheterostructures; strain-induced changes of the band structure[4,6,7] and effects caused by the new periodicity in the direction perpendicular to the layers of artificial superlattices are of special interest. Superlattice effects might lead to a quasidirect energy gap in the Si-Si_xGe_{1-x} system as proposed in Ref. 8. In the present Communication we discuss the observation of zone-folding effects on acoustic phonons in Si-Si_xGe_{1-x} periodic multilayer structures, which is the first direct evidence of superlattice effects in these strained layer systems. Raman scattering by folded-longitudinal-acoustic (LA) phonons has been reported previously for GaAs-$Al_xGa_{1-x}As$ (Refs. 9 and 10) and CdTe-$Cd_{1-x}Mn_xTe$ (Ref. 11) superlattices.

The samples used for the present studies were grown by molecular-beam epitaxy on [100]-oriented Si substrates. Details of the sample preparation and growth procedure are described elsewhere.[3] The layer sequence and the corresponding conduction- and valence-band edges are shown in Fig. 1. The proposed band offsets which are strongly influenced by built-in strains are discussed in Refs. 4 and 7. The buffer layer (thickness $\simeq 200$ nm) consists of either pure Si or $Si_{0.75}Ge_{0.25}$ alloy. It is followed by a periodic sequence of thin layers of Si and $Si_{0.5}Ge_{0.5}$. The total thickness of the superlattice is of the order of 100–200 nm. Various parameters of the different samples are listed in Table I. The $Si_{0.75}Ge_{0.25}$ buffer layer leads to a medium lattice spacing in between that of Si and $Si_{0.5}Ge_{0.5}$. It has been shown by Raman spectroscopy[4,12] that both types of superlattice layers are strained approximately to the same extent, but with opposite sign. In samples with Si buffer layers there is no strain in the Si layers, while it is doubled in the $Si_{0.5}Ge_{0.5}$ layers.[12]

Raman spectra were measured in backscattering geometry using a conventional Raman setup with double-grating spectrometer, GaAs photomultiplier, and photon-counting techniques. The penetration depth of the laser line used ($\lambda_L = 501.7$ nm) is about 500 nm. The scattering wave vector in the backscattering geometry is $q_s \simeq 2(2\pi n/\lambda_L)$, where n is the refractive index of the sample. For $\lambda_L \simeq 500$ nm, $n \simeq 4.33$ both for Si and Ge. Therefore, we assume that this value also holds for $Si_{0.5}Ge_{0.5}$. The resulting scattering wave vector amounts to $q_s = 1.085 \times 10^6$ cm^{-1}. A typical Raman spectrum of sample No. 3 is shown in Fig. 2. The information depth of about 500 nm allows us to probe phonon modes of the multilayer structure, of the buffer layer, and of the substrate. Information on composition, crystallinity, and built-in strain of the different layers can be extracted from the energy positions, intensities, and line shapes of the various optical modes. These properties are discussed in detail elsewhere.[4,12,13] In addition to the optical modes several sharp peaks are observed in the low-energy

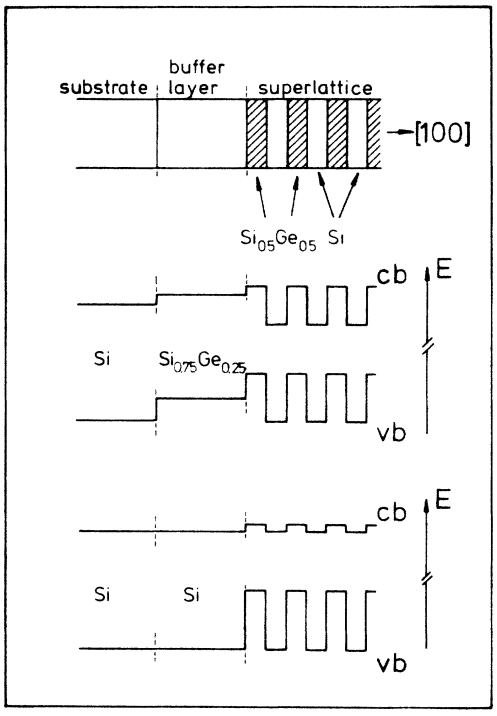

FIG. 1. Schematic illustration of Si-$Si_{0.5}Ge_{0.5}$ strained-layer superlattices. The proposed real-space energy diagrams of samples grown on different buffer layers are shown in the lower part (for details, see Ref. 7). vb denotes the valence band, ch the conduction band.

TABLE I. List of Si-$Si_{0.5}Ge_{0.5}$ strained-layer superlattices used in our experiments. The layers are equidistant: $d=2d_1$, $d_1=d_2$. ϵ denotes the percent of strain in the corresponding superlattice layers.

Sample	Buffer layer	ϵ (%) Si	ϵ (%) $Si_{0.5}Ge_{0.5}$	Superlattice period d (Å)	Number of periods
1	Si	0	−2	46	50
2	Si	0	−2	163	10
3	$Si_{0.75}Ge_{0.25}$	+1	−1	138	10

region of the spectrum. The two dominant ones shown in Fig. 2 are even stronger in intensity than the optical modes. The energy position of the doublet depends on layer thickness or superlattice period. In the following it is shown that the observed low-energy modes result from the Brillouin-zone folding of the acoustic-phonon spectrum due to the superlattice. The data are explained by a theory which treats the phonons in the elastic continuum limit similar to that used for GaAs-$Al_xGa_{1-x}As$ (Refs. 9 and 10) and CdTe-$Cd_{1-x}Mn_xTe$ (Ref. 11) superlattices. We use the energy position of the strongest doublet for an exact determination of the superlattice period $d=d_1+d_2=2d_1=2d_2$, where $d_1=d_2$ is the individual thickness of the Si and $Si_{0.5}Ge_{0.5}$ layers.

In the continuum limit the energy–wave-vector relation of acoustic vibrations in a layered structure is given by[14]

$$\cos(qd)=\cos\left(\frac{\omega d}{2v_1}\right)\cos\left(\frac{\omega d}{2v_2}\right)-\left(\frac{1+k^2}{2k}\right)\sin\left(\frac{\omega d}{2v_1}\right)\sin\left(\frac{\omega d}{2v_2}\right), \quad (1)$$

where v_1 and v_2 are the sound velocities of the two media, and $k=v_1\rho_1/v_2\rho_2$. ρ_1 and ρ_2 are the densities of the Si and $Si_{0.5}Ge_{0.5}$ layers, respectively. The parameters used to calculate the folded LA modes are

$$v_1(\mathrm{Si})=(c_{11}/\rho_1)^{1/2}=8.433\times10^5\ \mathrm{cm/s}\ ,$$

$$\rho_1(\mathrm{Si})=2.33\ \mathrm{g/cm^3}\ ,$$

$$\rho_2(Si_{0.5}Ge_{0.5})=[\rho(\mathrm{Si})+\rho(\mathrm{Ge})]/2=3.83\ \mathrm{g/cm^3}\ .$$

The sound velocity of $Si_{0.5}Ge_{0.5}$ is not known very well. There is some evidence that it is larger than expected from a linear interpolation between the Ge and Si values.[15] Information on $v_2(Si_{0.5}Ge_{0.5})$, however, is obtained directly from our measurements. It can be shown that for $d_1=d_2$ the average sound velocity in the superlattice is given by[10]

$$\frac{v}{v_1}=2\left[1+\frac{\rho_2}{\rho_1}+\left(\frac{v_1}{v_2}\right)^2\left(1+\frac{\rho_1}{\rho_2}\right)\right]^{-1/2}\ . \quad (2)$$

For a fixed scattering wave vector q_s, the average sound velocity v is directly related to the energy splitting of the observed doublets: $\Delta\omega=2q_sv$. $q_s=1.085\times10^6\ \mathrm{cm^{-1}}$ is fixed by the laser wavelength used and the scattering configuration. It turns out that the doublet splitting is independent of the superlattice period for $\pi/d>q_s$ and q_s away from the new Brillouin-zone boundary. In our experimental situation this corresponds to $d\lesssim25$ nm. The measured doublet splitting in samples 1–3 is indeed constant and amounts to $\Delta\omega\sim9\ \mathrm{cm^{-1}}$ (see Figs. 3 and 4). It corresponds to an average sound velocity $v=7.8\times10^5$ cm/s. From Eq. (2) we can now deduce the sound velocity which corresponds to the LA phonons in the strained $Si_{0.5}Ge_{0.5}$ layers. In agreement with Ref. 15, the resulting $v_2=(7.5\pm0.4)\times10^5$ cm/s is slightly higher than the value obtained from a linear interpolation between the Si and Ge values (6.7×10^5 cm/s).

The LA-phonon dispersion within the new superlattice Brillouin zone has been calculated with the fixed parameters for various periods. Figure 3 shows the result for $d=163$ Å. This period fits best the folded modes of sample 2. The three low-lying modes are dominant in the spectra. They agree very well with the calculated dispersion curves. The higher-energy modes are much weaker and are not included in the present evaluation. For unknown reasons the third doublet shows up stronger, especially in sample 2. The positions of those two peaks are also plotted in Fig. 3. They are slightly lower than expected from the calculated dispersion curves. This probably indicates the limit of the elastic continuum theory in this frequency range.

In Fig. 4 the calculated energy positions of the three low-energy modes are plotted versus superlattice period d for fixed $q_s=1.085\times10^6\ \mathrm{cm^{-1}}$. The first mode at 4.6 $\mathrm{cm^{-1}}$ is essentially independent of d and is determined by $\omega=q_sv$,

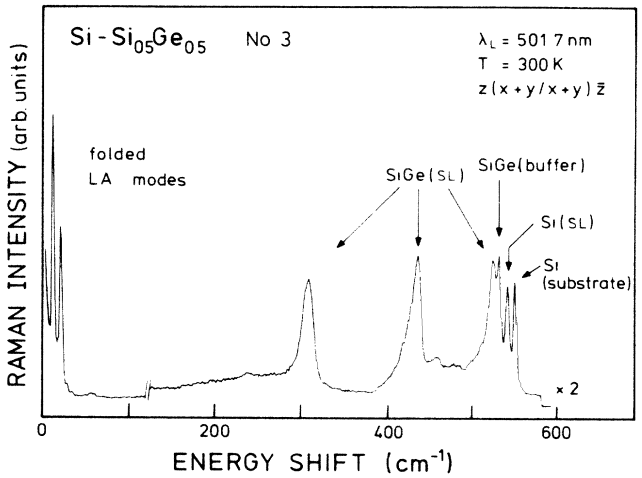

FIG. 2. Raman spectra of a Si-$Si_{0.5}Ge_{0.5}$ strained-layer superlattice grown on $Si_{0.75}Ge_{0.25}$ buffer layer. The arrows indicate the energy positions of optical-phonon modes originating from different layers [substrate, buffer layer, superlattice (SL)]. Additionally folded-LA phonons with high intensity appear in the low-energy part of the spectra.

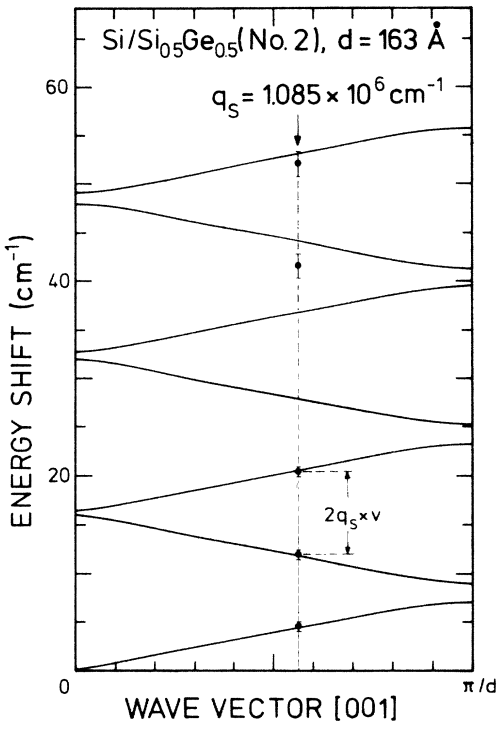

FIG. 3. Theoretical dispersion of longitudinal-acoustic (LA) phonons in the superlattice ($d = 163$ Å) based on the elastic continuum theory. Experimental frequencies are shown by dots (sample 2). q_s is fixed by the used laser line.

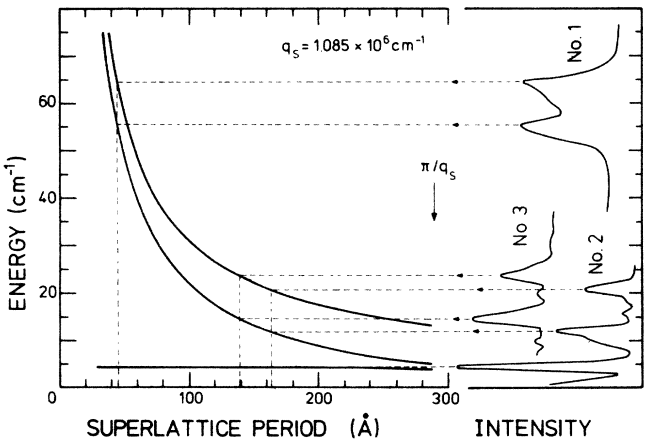

FIG. 4. Calculated frequencies for the first three eigenmodes of folded-LA phonons as a function of the superlattice period d. Corresponding Raman spectra are shown in the right part of the picture.

the product of the scattering wave vector and the average sound velocity. The other two modes represent the first strong doublet with a constant splitting $\Delta\omega = 2q_s v \sim 9$ cm^{-1} and whose energetic position is strongly dependent on d. The right-hand side of Fig. 4 shows three spectra of different samples measured with high-energy resolution ($\simeq 0.3$ cm^{-1}). All samples exhibit the mode at 4.6 cm^{-1}. The folded-LA-phonon doublet shifts to higher energy with decreasing layer thickness. By comparing the positions with the calculated energies we determine the superlattice periods to be $d = 46$ Å (No. 1), 138 Å (No. 3), and 163 Å (No. 2). In addition to the strong doublets, weaker peaks are observed in between and as shoulders. These structures are probably caused by folded-transverse-acoustic (TA) phonons, an assignment which is based on the good agreement of the measured positions with calculations. Scattering by transverse modes is basically not allowed in backscattering from [100] surfaces. However, the reduced symmetry due to the tetragonal distortion in the layers might cause a violation of the selection rules.

In conclusion, we have observed zone-folding effects on the acoustic-phonon branches of Si-$Si_{0.5}Ge_{0.5}$ strained-layer superlattices. The dispersion of the LA-phonon modes within the reduced one-dimensional Brillouin zone is well described by treating the phonons in the elastic continuum limit. The splitting of the observed doublet determines the average sound velocity in the multilayer structure. The energy position depends strongly on the superlattice period d. In addition, higher-energy doublets and weak structures caused by folded-TA phonons are observed. For a complete understanding it is necessary to evaluate the selection rules systematically. A change of the laser wavelength should also allow an experimental determination of the dispersion curves. Such work is in progress.

Part of this work has been supported by the Deutsche Forschungsgemeinschaft via Sonderforschungsberesch No. 128.

[1]E. Kasper and H. J. Herzog, Appl. Phys. **8**, 199 (1975).
[2]J. C. Bean, L. C. Feldman, A. T. Fiory, S. Nakahara, and J. K. Robinson, J. Vac. Sci. Technol. A **2**, 436 (1984).
[3]H. Jorke and H. J. Herzog, in *Proceedings of the First International Symposium on Silicon Molecular-Beam Epitaxy, 1985,* edited by J. C. Bean (Electrochemical Society, Pennington, 1985), p. 352.
[4]G. Abstreiter, H. Brugger, T. Wolf, H. J. Jorke, and H. J. Herzog, Phys. Rev. Lett. **54**, 2441 (1985).
[5]R. People, J. C. Bean, D. V. Lang, A. M. Sergent, H. L. Störmer, K. W. Wecht, R. T. Lynch, and K. Baldwin, Appl. Phys. Lett. **45**, 1231 (1984).
[6]R. People, Phys. Rev. B **32**, 1405 (1985).
[7]C. Zeller and G. Abstreiter, Z. Phys. (to be published); R. Zachai, T. Wolf, and G. Abstreiter (unpublished).
[8]U. Gnutzmann and K. Clausecker, Appl. Phys. **3**, 9 (1974).
[9]C. Colvard, R. Merlin, M. V. Klein, and A. C. Gossard, Phys. Rev. Lett. **45**, 298 (1980).
[10]J. Sapriel, J. C. Michel, J. C. Tolédano, R. Vacher, J. Kervarec, and A. Regreny, Phys. Rev. B **28**, 2007 (1983).
[11]S. Venugopalan, L. A. Kolodziejski, R. L. Gunshor, and A. K. Ramdas, Appl. Phys. Lett. **45**, 974 (1984).
[12]G. Abstreiter, H. Brugger, T. Wolf, H. Jorke, and H. J. Herzog, in *Proceedings of the Second International Conference on Modulated Semiconductor Structures, Kyoto, 1985,* edited by H. Sakaki [Surf. Science (to be published)]; E. Kasper, *ibid.* (to be published).
[13]F. Cerdeira, A. Pinczuk, J. C. Bean, B. Batlogg, and B. A. Wilson, Appl. Phys. Lett. **45**, 1138 (1984).
[14]S. M. Rytov, Akust. Zh. **2**, 71 (1956) [Sov. Phys. Acoust. **2**, 68 (1956)].
[15]V. T. Bublik, S. S. Gorelik, A. A. Zaitsev, and A. Y. Polyakov, Phys. Status Solidi B **66**, 427 (1974).